

A DETAILED NUMERICAL STUDY ON GENERALIZED ROSENAU-KDV EQUATION WITH FINITE ELEMENT METHOD

SEYDI BATTAL GAZI KARAKOC¹

Manuscript received: 23.05.2018; Accepted paper: 11.10.2018;

Published online: 30.12.2018.

Abstract. In this study, we have got numerical solutions of the generalized Rosenau-KdV equation by using collocation finite element method in which septic B-splines are used as approximate functions. Effectivity and proficiency of the method are shown by solving the equation with different initial and boundary conditions. Also, to do this L_2 and L_∞ error norms and two lowest invariants I_M and I_E have been computed. A linear stability analysis indicates that our algorithm, based on a Crank Nicolson approximation in time, is unconditionally stable. An error analysis of the new algorithm has been made. The obtained numerical solutions are compared with some earlier studies. This comparison clearly indicates that the obtained results are better than the earlier results.

Keywords: Generalized Rosenau KdV equation, finite element method, collocation, septic B-spline, soliton.

1. INTRODUCTION

In this article, we will conceive the following generalized Rosenau-KdV equation

$$U_t + \alpha U_x + \beta U_{xxx} + \varepsilon U_{xxxx} + (U^p)_x = 0, \quad (0.1)$$

with the homogeneous boundary conditions,

$$\begin{aligned} U(a,t) &= 0, & U(b,t) &= 0, \\ U_x(a,t) &= 0, & U_x(b,t) &= 0, \\ U_{xx}(a,t) &= 0, & U_{xx}(b,t) &= 0, \quad t > 0 \end{aligned} \quad (0.2)$$

and an initial condition

$$U(x,0) = f(x) \quad a \leq x \leq b, \quad (0.3)$$

where $p \geq 2$ is an integer, U_{xxx} is the viscous term and subscripts x and t denote differentiation. The following usual Rosenau-KdV equation

$$U_t + \alpha U_x + \beta U_{xxx} + \varepsilon U_{xxxx} + UU_x = 0, \quad (0.4)$$

¹ Nevsehir Haci Baktas Veli University, Faculty of Science and Art, Department of Mathematics, 50300 Nevsehir, Turkey. E-mail: sbgk44@gmail.com.

is obtained by taking $p = 2$ in Eq.(1.1). Up to now, many computation techniques have been presented on the Rosenau-KdV equation. Zuo, used the sine-cosine and the tanh methods for solving the Rosenau-KdV equation [1]. A conservative three-level linear finite difference scheme for the numerical solution of the initial-boundary value problem of Rosenau-KdV equation is suggested by J. Hu et al [2]. The topological soliton solution or shock wave solutions of this equation were analyzed by G. Ebadi et al [3]. The 1-soliton solution is got by the ansatz method for solitary waves and singular solitons and the soliton perturbation theory is performed to define the adiabatic dynamics of the perturbed soliton by Razborova et al [4]. B. Wongsaijai and K. Poochinapan [5] proposed a mathematical model to obtain the solution of the nonlinear wave by coupling the Rosenau-KdV equation. In [6,7] authors solved the equation with subdomain finite element method based on the sextic B-spline basis functions and collocation finite element method, respectively. Until now, numerical method for the initial-boundary value problem of the generalized Rosenau-KdV equation has not been studied widely. N. Atouani and K. Omrani [8] examined two conservative finite difference schemes for the Rosenau-KdV equation (1.4) in 2D. A. Esfahani [9] obtained the solitary wave solutions of the generalized Rosenau-KdV equation with sech-ansatze method and also gave the two invariants for the generalized Rosenau-KdV equation. An average linear finite difference scheme for the numerical solution of the initial-boundary value problem of generalized Rosenau-KdV equation was studied by M. Zheng and J. Zhou [10]. Y. Luo et al. [11] proposed a conservative Crank-Nicolson finite difference scheme for the initial-boundary value problem of the generalized Rosenau-KdV equation. The following KdV equation

$$U_t + aUU_x + bU_{xxx} = 0, \quad (0.5)$$

has a number of shortcomings [12, 13]. Such as, first one, it defines an unidirectional propagation of waves. Therefore, it can not describe the wave-wave and wave-wall interactions. Second one, since it was obtained under the assumption of weak an harmonicity, shape and the behavior of the high amplitude waves can not be well predicted by the KdV equation [14]. To cope with the shortcoming of the Eq. (1.5), the following Rosenau equation

$$U_t + U_x + U_{xxxxt} + (U^2)_x = 0, \quad (0.6)$$

was proposed by Rosenau [15, 16]. M. A. Park examined existence and uniqueness and regularity of the solutions for the Rosenau equation [17].

In this study, we have constructed the septic B-spline collocation method to the generalized Rosenau-KdV equation. Our study is designed as follows: numerical algorithm is expressed in Section 2. Stability and error analysis of the scheme are considered in Section 3 and 4. Numerical examples and results are discussed in Section 5. In the final section, a conclusion is given.

2. SEPTIC B-SPLINE COLLOCATION METHOD

For the numerical calculation, solution domain of the problem is limited over an interval $a \leq x \leq b$. The interval $[a, b]$ is divided into N equal subinterval by the points x_m such that $a = x_0 < x_1 < \dots < x_{N-1} < x_N = b$ and $h = \frac{b-a}{N} = x_{m+1} - x_m$. The set of septic

B-spline functions $\varphi_m(x) (m = -3(1)N + 3)$ form a basis over the solution region $[a, b]$. The numerical solution $U_N(x, t)$ is expressed in terms of the septic B-splines as

$$U_N(x, t) = \sum_{m=-3}^{N+3} \varphi_m(x) \delta_m(t). \tag{0.7}$$

Septic B-splines $\varphi_m(x)$ at the knots x_m are designed over the interval $[a, b]$ by Prenter [18]

$$\varphi_m(x) = \frac{1}{h^7} \begin{cases} (x - x_{m-4})^7 & [x_{m-4}, x_{m-3}] \\ (x - x_{m-4})^7 - 8(x - x_{m-3})^7 & [x_{m-3}, x_{m-2}] \\ (x - x_{m-4})^7 - 8(x - x_{m-3})^7 + 28(x - x_{m-2})^7 & [x_{m-2}, x_{m-1}] \\ (x - x_{m-4})^7 - 8(x - x_{m-3})^7 + 28(x - x_{m-2})^7 - 56(x - x_{m-1})^7 & [x_{m-1}, x_m] \\ (x_{m+4} - x)^7 - 8(x_{m+3} - x)^7 + 28(x_{m+2} - x)^7 - 56(x_{m+1} - x)^7 & [x_m, x_{m+1}] \\ (x_{m+4} - x)^7 - 8(x_{m+3} - x)^7 + 28(x_{m+2} - x)^7 & [x_{m+1}, x_{m+2}] \\ (x_{m+4} - x)^7 - 8(x_{m+3} - x)^7 & [x_{m+2}, x_{m+3}] \\ (x_{m+4} - x)^7 & [x_{m+3}, x_{m+4}] \\ 0 & otherwise. \end{cases} \tag{0.8}$$

A characteristic finite interval $[x_m, x_{m+1}]$ is matched to the interval $[0, 1]$ by a local coordinate transformation defined by $h\xi = x - x_m$, $0 \leq \xi \leq 1$. Hence septic B-splines (2.2) in terms of ξ over $[0, 1]$ can be given as follows:

$$\begin{aligned} \varphi_{m-3} &= 1 - 7\xi + 21\xi^2 - 35\xi^3 + 35\xi^4 - 21\xi^5 + 7\xi^6 - \xi^7, \\ \varphi_{m-2} &= 120 - 392\xi + 504\xi^2 - 280\xi^3 + 84\xi^5 - 42\xi^6 + 7\xi^7, \\ \varphi_{m-1} &= 1191 - 1715\xi + 315\xi^2 + 665\xi^3 - 315\xi^4 - 105\xi^5 + 105\xi^6 - 21\xi^7, \\ \varphi_m &= 2416 - 1680\xi + 560\xi^4 - 140\xi^6 + 35\xi^7, \\ \varphi_{m+1} &= 1191 + 1715\xi + 315\xi^2 - 665\xi^3 - 315\xi^4 + 105\xi^5 + 105\xi^6 - 35\xi^7, \\ \varphi_{m+2} &= 120 + 392\xi + 504\xi^2 + 280\xi^3 - 84\xi^5 - 42\xi^6 + 21\xi^7, \\ \varphi_{m+3} &= 1 + 7\xi + 21\xi^2 + 35\xi^3 + 35\xi^4 + 21\xi^5 + 7\xi^6 - \xi^7, \\ \varphi_{m+4} &= \xi^7. \end{aligned} \tag{0.9}$$

For the problem, the finite elements are identified with the interval $[x_m, x_{m+1}]$. Using Eq.(2.1) and Eq.(2.2), the nodal values of $U_m, U'_m, U''_m, U'''_m, U_m^{iv}$ are given in terms of the element parameters δ_m by

$$\begin{aligned} U_N(x_m, t) &= U_m = \delta_{m-3} + 120\delta_{m-2} + 1191\delta_{m-1} + 2416\delta_m + 1191\delta_{m+1} + 120\delta_{m+2} + \delta_{m+3}, \\ U'_m &= \frac{7}{h}(-\delta_{m-3} - 56\delta_{m-2} - 245\delta_{m-1} + 245\delta_{m+1} + 56\delta_{m+2} + \delta_{m+3}), \\ U''_m &= \frac{42}{h^2}(\delta_{m-3} + 24\delta_{m-2} + 15\delta_{m-1} - 80\delta_m + 15\delta_{m+1} + 24\delta_{m+2} + \delta_{m+3}), \\ U'''_m &= \frac{210}{h^3}(-\delta_{m-3} - 8\delta_{m-2} + 19\delta_{m-1} - 19\delta_{m+1} + 8\delta_{m+2} + \delta_{m+3}), \\ U_m^{iv} &= \frac{840}{h^4}(\delta_{m-3} - 9\delta_{m-1} + 16\delta_m - 9\delta_{m+1} + \delta_{m+3}) \end{aligned} \tag{0.10}$$

and the variation of U over the element $[x_m, x_{m+1}]$ is given by [19]

$$U = \sum_{m=-3}^{N+3} \varphi_m \delta_m. \quad (0.11)$$

When we identify the collocation points with the knots and use Eqs.(2.4) to evaluate U_m , its space derivatives and substitute into Eq.(1.1); this leads to a set of ordinary differential equations of the form

$$\begin{aligned} & \dot{\delta}_{m-3} + 120\dot{\delta}_{m-2} + 1191\dot{\delta}_{m-1} + 2416\dot{\delta}_m + 1191\dot{\delta}_{m+1} + 120\dot{\delta}_{m+2} + \dot{\delta}_{m+3} \\ & + \frac{7\alpha}{h} (-\delta_{m-3} - 56\delta_{m-2} - 245\delta_{m-1} + 245\delta_{m+1} + 56\delta_{m+2} + \delta_{m+3}) \\ & + \frac{210\beta}{h^3} (-\delta_{m-3} - 8\delta_{m-2} + 19\delta_{m-1} - 19\delta_{m+1} + 8\delta_{m+2} + \delta_{m+3}) \\ & + \frac{840\varepsilon}{h^4} (\dot{\delta}_{m-3} - 9\dot{\delta}_{m-1} + 16\dot{\delta}_m - 9\dot{\delta}_{m+1} + \dot{\delta}_{m+3}) \\ & + p \frac{7}{h} Z_m (-\delta_{m-3} - 56\delta_{m-2} - 245\delta_{m-1} + 245\delta_{m+1} + 56\delta_{m+2} + \delta_{m+3}) = 0, \end{aligned} \quad (0.12)$$

where $Z_m = (\delta_{m-3} + 120\delta_{m-2} + 1191\delta_{m-1} + 2416\delta_m + 1191\delta_{m+1} + 120\delta_{m+2} + \delta_{m+3})^{p-1}$.

If δ_i and its time derivatives $\dot{\delta}_i$ in Eq.(2.6) are decoupled by the Crank-Nicolson formula

$$\delta_i = \frac{\delta_i^{n+1} + \delta_i^n}{2}, \quad (0.13)$$

and usual finite difference approximation

$$\dot{\delta}_i = \frac{\delta_i^{n+1} - \delta_i^n}{\Delta t} \quad (0.14)$$

we derive a repetition relationship between two time levels n and $n+1$ relating two unknown parameters δ_i^{n+1} , δ_i^n for $i = m-3, m-2, \dots, m+2, m+3$

$$\begin{aligned} & \gamma_1 \delta_{m-3}^{n+1} + \gamma_2 \delta_{m-2}^{n+1} + \gamma_3 \delta_{m-1}^{n+1} + \gamma_4 \delta_m^{n+1} + \gamma_5 \delta_{m+1}^{n+1} + \gamma_6 \delta_{m+2}^{n+1} + \gamma_7 \delta_{m+3}^{n+1} \\ & = \gamma_7 \delta_{m-3}^n + \gamma_6 \delta_{m-2}^n + \gamma_5 \delta_{m-1}^n + \gamma_4 \delta_m^n + \gamma_3 \delta_{m+1}^n + \gamma_2 \delta_{m+2}^n + \gamma_1 \delta_{m+3}^n, \end{aligned} \quad (0.15)$$

where

$$\begin{aligned} \gamma_1 &= [1 - E(\alpha + pZ_m) - M + K], \\ \gamma_2 &= [120 - 56E(\alpha + pZ_m) - 8M], \\ \gamma_3 &= [1191 - 245E(\alpha + pZ_m) + 19M - 9K], \\ \gamma_4 &= [2416 + 16K], \\ \gamma_5 &= [1191 + 245E(\alpha + pZ_m) - 19M - 9K], \\ \gamma_6 &= [120 + 56E(\alpha + pZ_m) + 8M], \\ \gamma_7 &= [1 + E(\alpha + pZ_m) + M + K], \\ m &= 0, 1, \dots, N, \quad E = \frac{7}{2h} \Delta t, \quad M = \frac{105\beta}{h^3} \Delta t, \quad K = \frac{840\varepsilon}{h^4} \Delta t. \end{aligned} \quad (0.16)$$

The system (2.9) involves of $(N+1)$ linear equations containing $(N+7)$ coefficients $(\delta_{-3}, \delta_{-2}, \delta_{-1}, \dots, \delta_{N+1}, \delta_{N+2}, \delta_{N+3})^T$. We need six additional restraints to obtain a unique solution for this system. These are obtained from the boundary conditions (1.2) and can be used to

where σ is mode number h is the element size, $\theta = \sigma h$

$$\begin{aligned}\eta_1 &= 1 - \alpha_1 - \alpha_2 + \alpha_3, & \eta_2 &= 120 - 56\alpha_1 - 8\alpha_2, \\ \eta_3 &= 1191 - 245\alpha_1 + 19\alpha_2 - 9\alpha_3, & \eta_4 &= 2416 + 16\alpha_3, \\ \eta_5 &= 1191 + 245\alpha_1 - 19\alpha_2 - 9\alpha_3, & \eta_6 &= 120 + 56\alpha_1 + 8\alpha_2, \\ \eta_7 &= 1 + \alpha_1 + \alpha_2 + \alpha_3, & m &= 0, 1, \dots, N, \quad \alpha_1 = \frac{7\Delta t}{2h}(\alpha + Z_m), \quad \alpha_2 = \frac{210\beta\Delta t}{2h^3}, \quad \alpha_3 = \frac{840\varepsilon}{h^4}.\end{aligned}$$

If we simplify the Eq. (2.12),

$$\xi = \frac{A - iB}{A + iB}$$

is obtained where

$$\begin{aligned}A &= (2382 - 18\alpha_3)\cos(\theta) + 240\cos(2\theta) + (2 + 2\alpha_3)\cos(3\theta) + (2416 + 16\alpha_3), \\ B &= (490\alpha_1 - 2\alpha_2)\sin(\theta) + (112\alpha_1 + 16\alpha_2)\sin(2\theta) + (490\alpha_1 - 38\alpha_2)\sin(3\theta) \\ \alpha_1 &= E(\alpha + pZ_m) \quad , \quad \alpha_2 = M \quad , \quad \alpha_3 = K \quad , \quad m = 0, 1, \dots, N - 1.\end{aligned}$$

The modulus of $|\xi|$ is 1, so the linearized scheme is unconditionally stable.

4. ERROR ANALYSIS

In this study, we choose septic B-spline collocation algorithm to obtain the numerical solution of the generalized Rosenau-KdV equation. Since it provides perfect convergence pointwise and does not contain an integral expression, we use the collocation algorithm. Let $H^r(\Omega)$ be the space of r times differentiable functions and $\|\cdot\|_r$ be the standard $H^r(\Omega)$ norm. v_h is an approximation to a function $v(x) \in H^r(\Omega)$ in Ω , h is the element size and $\Omega = \cup_i \Omega_i$ where $\Omega_i = [x_i, x_{i+1}]$, $x_{i+1} = x_i + h$. We notice [21, 22] that $\|v(x) - v_h(x)\| \leq Ch^{k+1} \|v\|_{k+1}$ where $1 \leq k < r$ and v_h represents interpolation by piecewise-polynomials of degree r ($\Omega = \cup_i \Omega_i$) [7]. The error is conserved with the Galerkin finite element method equally [20] if w_h is an appropriate B-splines identified with a polynomial of degree less or equal k then $\|w(x) - w_h(x)\| \leq C\Delta x^{l+1} \|w\|_{l+1}$, where $1 \leq l < k$, for any $w \in H_k(\Omega)$. For our work we choose septic B-splines for space integration. So these inequalities offer $\mathcal{O}(h^8)$ precision for the spatial approximation in $L_2(\Omega)$ norm. Hence for time variable, Crank-Nicolson formula is used which is of $\mathcal{O}(\Delta t^2)$ accurate in $L_2([0, T])$ norm for some $T > 0$; followed by a forward difference algorithm which is accurate of $\mathcal{O}(\Delta t)$ accurate in $L_2([0, T])$ norm for some $T > 0$ [22]. Therefore we get the limit of error as $\|u(x, t) - u_h(x, t)\| \leq C_1 h^8 + C_2 \Delta t^2 + C_3 \Delta t = C_1 h^8 + C_2 \Delta t$, for a proper $C_1 \geq 0$ and $C_2 \geq 0$ [7].

5. NUMERICAL SIMULATIONS

There are two conserved quantities for the generalized Rosenau-KdV equation. These are given by

$$I_M = \int_a^b U(x, t) dx,$$

$$I_E = \int_a^b [U^2(x, t) + \varepsilon U_{xx}^2(x, t)] dx$$

which correspond to the momentum and energy of the shallow water waves, respectively [9]. To see how precise the numerical algorithm estimates the position and amplitude of the solution as the simulation progresses, we use the following error norms:

$$L_2 = \|U^{exact} - U_N\|_2 \approx \sqrt{h \sum_{j=0}^N |U_j^{exact} - (U_N)_j|^2}$$

and the error norm

$$L_\infty = \|U^{exact} - U_N\|_\infty \approx \max_j |U_j^{exact} - (U_N)_j|.$$

To show the efficiency of the method, we have focused on searching solitary wave solutions of the Eq. (1.1).

5.1. THE SOLITON SOLUTIONS OF SINGLE WAVE

In this section, different numerical examples will be given to illustrate the efficiency and accuracy of the method. For the numerical simulations of the movement of single solitary wave, three sets of parameters have been used and discussed.

5.1.1. CASE 1.

For the first case, we have used the parameters $p=2$, $\alpha=1$, $\beta=1$, $\varepsilon=1$ over the interval $[-60, 90]$. For this set the exact solution of the equation is given as [7]

$$U(x, t) = \left(-\frac{35}{24} + \frac{35}{312}\sqrt{313}\right) \operatorname{sech}^4\left[\frac{1}{24}\sqrt{-26 + 2\sqrt{313}}\left(x - \left(\frac{1}{2} + \frac{1}{26}\sqrt{313}\right)t\right)\right],$$

with the boundary conditions $U \rightarrow 0$ as $x \rightarrow \pm\infty$ and the initial condition

$$U(x, 0) = \left(-\frac{35}{24} + \frac{35}{312}\sqrt{313}\right) \operatorname{sech}^4\left[\frac{1}{24}\sqrt{-26 + 2\sqrt{313}}x\right].$$

The computations are done until time $t=40$ to find the error norms L_2, L_∞ and invariants I_M, I_E . The amplitude and velocity of solitary wave are obtained as 0.526057, $v=1.180454$ respectively. The calculated quantities of the invariants and errors are presented in Table (1). The percentage of the relative error of the preserved quantities I_M and I_E are computed according to the preserved quantities at $t=0$. The percentage of relative changes of

I_M and I_E are found to be $9.4 \times 10^{-7}\%$ and $1.5 \times 10^{-9}\%$ for $h = \Delta t = 0.1$; $1.1 \times 10^{-6}\%$ and 0 for $h = \Delta t = 0.125$; $5.5 \times 10^{-7}\%$ and $1 \times 10^{-7}\%$ for $h = \Delta t = 0.025$, respectively. It is clearly seen that the invariants remain almost stable during the computer programme run. We can easily see from Table (1) that the invariant I_M changes from its initial value by less than 1×10^{-9} whereas the changes of invariant I_E approach to zero throughout for different values of h and Δt . Also, we have found out error norms L_2 and L_∞ are obtained adequately small during the computer run. So, we can say our method is reasonable conservative. In Table 2, we compare the values of the error norms obtained by the current method with methods obtained by J. Hu et al. [2] and T. Ak et al. [6]. In this table, we alleged that the error norms obtained by our method are much better or found in good agreement with the others. Simulations of single soliton time up to $t = 40$ are given in Figure (1). We observed from the Figure (1), single soliton travels to the right at a constant speed and preserves its amplitude and shape with increasing time unsurprisingly. The amplitude is 0.526057 at $t = 0$ and located at $x = -0.125$, while it is 0.526146 at $t = 40$ and located at $x = 47.250$. The absolute difference in amplitudes at times $t = 0$ and $t = 40$ is 8.9×10^{-5} so that there is a little change between amplitudes. Error values between analytical and numerical solutions are demonstrated in Table 2.

Table 1. The invariants and the error norms for single solitary wave with $p = 2$, $\alpha = 1$, $\beta = 1$, $\varepsilon = 1$.

$h = \Delta t = 0.1$	I_M	I_E	$L_2 \times 10^{-4}$	$L_\infty \times 10^{-4}$
t				
0	5.4981750556	1.9897841614	0	0
10	5.4981750556	1.9897841614	3.56724	1.41640
20	5.4981750556	1.9897841614	6.46705	2.44374
30	5.4981750572	1.9897841614	9.02514	3.26169
40	5.4981750037	1.9897841614	11.62488	4.11491
$h = \Delta t = 0.125$	I_M	I_E	$L_2 \times 10^{-4}$	$L_\infty \times 10^{-4}$
t				
0	5.4981740747	1.9897835319	0	0
10	5.4981740747	1.9897835319	5.60011	2.20715
20	5.4981740746	1.9897835319	10.26734	3.86253
30	5.4981740787	1.9897835319	14.22670	5.19178
40	5.4981740130	1.9897835319	17.73066	6.33780
$h = \Delta t = 0.025$	I_M	I_E	$L_2 \times 10^{-4}$	$L_\infty \times 10^{-4}$
t				
0	5.4981698357	1.9897809062	0	0
10	5.4981698363	1.9897809076	0.35170	0.14206
20	5.4981698379	1.9897809079	0.91672	0.32589
30	5.4981698426	1.9897809085	1.04343	0.46813
40	5.4981698357	1.9897809062	1.18321	0.48477

Table 2. Comparison of error norms with $p = 2, \alpha = 1, \beta = 1, \varepsilon = 1$ and different values of h and Δt at time $t = 40$.

$h = \Delta t = 0.1$	$L_2 \times 10^{-3}$			$L_\infty \times 10^{-3}$		
t	Present	[2]	[6]	Present	[2]	[6]
0	0.000000	0.000000	0.000000	0.000000	0.000000	0.000000
10	0.356723	1.641934	0.356724	0.141640	0.631419	0.141639
20	0.646705	3.045414	0.646705	0.244374	1.131442	0.244374
30	0.902514	4.241827	0.902514	0.326169	1.533771	0.326169
40	1.162488	5.297873	1.162489	0.411491	1.878952	0.411492
$h = \Delta t = 0.125$	$L_2 \times 10^{-4}$			$L_\infty \times 10^{-4}$		
t	Present	[2]	[6]	Present	[2]	[6]
0	0.000000	0.000000	0.000000	0.000000	0.000000	0.000000
10	5.60011	4.113510	0.854386	2.20715	1.582641	0.343706
20	10.26734	7.631169	1.779040	3.86253	2.835874	0.627075
30	14.22670	10.62971	2.810186	5.19178	3.843906	0.975412
40	17.73066	13.27645	3.783328	6.33780	4.709118	1.293116
$h = \Delta t = 0.025$	$L_2 \times 10^{-4}$			$L_\infty \times 10^{-5}$		
t	Present	[2]	[6]	Present	[2]	[6]
0	0.000000	0.000000	0.000000	0.000000	0.000000	0.000000
10	0.357059	1.028173	0.351702	1.421479	3.965867	1.420544
20	0.925408	1.905450	0.916735	3.264848	7.097948	3.258903
30	1.057023	2.650990	1.043479	4.742297	9.610332	4.681364
40	1.183710	3.306738	1.183139	4.846861	11.76011	4.847163

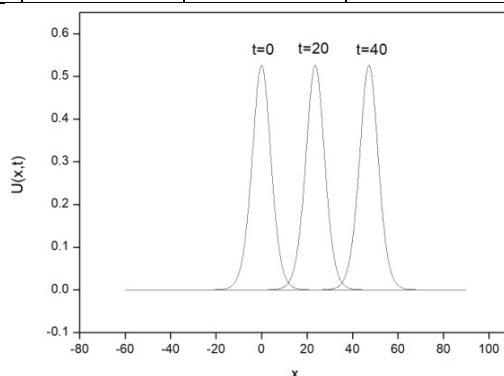


Figure 1. Motion of single solitary wave for $p = 2, \alpha = 1, \beta = 1, \varepsilon = 1, h = \Delta t = 0.125$ over the interval $[-60; 90]$ at specified times.

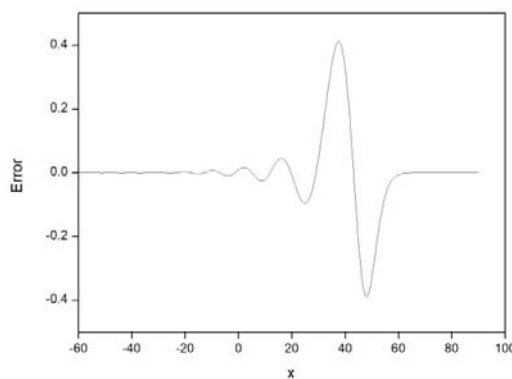


Figure 2. Absolute error for $p = 2, \alpha = 1, \beta = 1, \varepsilon = 1, h = \Delta t = 0.125$ at $t = 40$.

5.1.2. CASE 2

For the second case, we have chosen the parameters $p = 3$, $\alpha = 1$, $\beta = 1$, $\varepsilon = 1$ over the interval $[-60, 90]$. For this set the exact solution of the equation can be found as [4, 9]

$$U(x, t) = \frac{1}{4} \sqrt{-15 + 3\sqrt{41}} \operatorname{sech}^2 \frac{1}{4} \sqrt{\frac{-5 + \sqrt{41}}{2}} \left[x - \frac{1}{10} (5 + \sqrt{41}) t \right].$$

We examine the equation with the boundary conditions $U \rightarrow 0$ as $x \rightarrow \pm\infty$ and the initial condition

$$U(x, 0) = \frac{1}{4} \sqrt{-15 + 3\sqrt{41}} \operatorname{sech}^2 \frac{1}{4} \sqrt{\frac{-5 + \sqrt{41}}{2}} x.$$

For these parameters amplitude and velocity of solitary wave are found as 0.512568, $v = 1.140312$, respectively. The computations are done until time $t = 40$. The obtained results are listed in Table (3). The percentage of the relative error of the preserved quantities I_M and I_E are computed with respect to the preserved quantities at $t = 0$. The percentage of relative changes of I_M and I_E are found to be $9.6 \times 10^{-8}\%$ and $3.5 \times 10^{-8}\%$ when $h = \Delta t = 0.25$; $2.8 \times 10^{-8}\%$ and $8.8 \times 10^{-9}\%$ when $h = \Delta t = 0.125$; $6.0 \times 10^{-9}\%$ and $2.2 \times 10^{-9}\%$ when $h = \Delta t = 0.0625$, respectively. Table (3) shows that invariants are almost constant as the time increases. It is noticeably seen from the table that the invariants I_M and I_E change from their initial value by less than 1×10^{-8} for different values of h and Δt . Also, we have found out error norms L_2 and L_∞ are obtained sufficiently small during the computer run. Therefore our method is sensibly conservative. We compare the values of the error norms obtained by the current method with methods obtained by M. Zheng et al. [10] and Y. Luo et al. [11] in Table (4). This table clearly shows that the error norms obtained by our method are much better than the others. In Table (5) we compare values of the I_E with results from obtained by [11]. From this table, we can conclude that the values of the invariants are to be close to each other. For visual representation, the simulations of single soliton for values of $h = \Delta t = 0.125$ at times $t = 0, 20$ and 40 are illustrated in Figure (3). It is understood from this figure that the numerical scheme performs the motion of propagation of a single solitary wave, which moves to the right at nearly unchanged speed and conserves its amplitude and shape with increasing time. The amplitude is 0.512568 at $t = 0$ and located at $x = -0.125$, while it is 0.512741 at $t = 40$ and located at $x = 45.625$. The absolute difference in amplitudes at times $t = 0$ and $t = 40$ is 1.7×10^{-4} so there is a little change between amplitudes. Error distribution at time $t = 40$ is depicted graphically in Figure (4). As it is seen, the maximum errors occur around the central position of the solitary wave.

Table 3. The invariants and the error norms for single solitary wave with $p = 3, \alpha = 1, \beta = 1, \varepsilon = 1$.

$h = \Delta t = 0.1$	I_M	I_E	$L_2 \times 10^{-3}$	$L_\infty \times 10^{-3}$
t				
0	4.8989798241	1.6825480773	0	0
10	4.8989798239	1.6825480773	2.880540	1.166531
20	4.8989798231	1.6825480773	5.325785	2.035358
30	4.8989798678	1.6825480773	7.552481	2.800947
40	4.8989785482	1.6825480773	9.670753	3.516945
$h = \Delta t = 0.125$				
t				
0	4.8989798241	1.6825480772	0	0
10	4.8989798239	1.6825480772	0.721967	0.292411
20	4.8989798235	1.6825480772	1.335453	0.510960
30	4.8989798344	1.6825480772	1.894530	0.702865
40	4.8989794651	1.6825480772	2.426625	0.883243
$h = \Delta t = 0.025$				
t				
0	4.8989798241	1.6825480772	0	0
10	4.8989798238	1.6825480771	0.180543	0.073127
20	4.8989798236	1.6825480772	0.333994	0.127801
30	4.8989798359	1.6825480773	0.473859	0.175815
40	4.8989796887	1.6825480774	0.606988	0.221008

Table 4. Comparison of error norms with $p = 3, \alpha = 1, \beta = 1, \varepsilon = 1$ and different values of h and Δt at time $t = 40$.

	$L_\infty \times 10^{-3}$		
	Present	[10]	[11]
$h = \Delta t = 0.25$	3.51694	13.4986	7.53941
$h = \Delta t = 0.125$	0.88324	3.42489	1.89987
$h = \Delta t = 0.0625$	0.22100	0.85957	0.47587

Table 5. Comparison of I_E with $p = 3, \alpha = 1, \beta = 1, \varepsilon = 1$ and different values of h and Δt .

$h = \Delta t = 0.25$	I_E	I_E
t	Present	[11]
0	1.6825480773	1.68252899330
10	1.6825480773	1.68252899329
20	1.6825480773	1.68252899328
30	1.6825480773	1.68252899327
40	1.6825480773	1.68252899325

Table 5. (continued)

$h = \Delta t = 0.125$		
t	Present	[11]
0	1.6825480772	1.68254308255
10	1.6825480773	1.68254308255
20	1.6825480772	1.68254308255
30	1.6825480772	1.68254308255
40	1.6825480772	1.68254308254
$h = \Delta t = 0.0625$		
t	Present	[11]
0	1.6825480772	1.68254661109
10	1.6825480771	1.68254661108
20	1.6825480772	1.68254661095
30	1.6825480773	1.68254661102
40	1.6825480774	1.68254661095

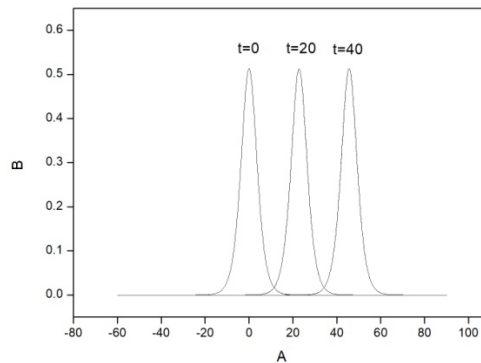


Figure 3. Motion of single solitary wave for $p = 3$, $\alpha = 1$, $\beta = 1$, $\varepsilon = 1$, $h = \Delta t = 0.125$ over the interval $[-60; 90]$ at specified times.

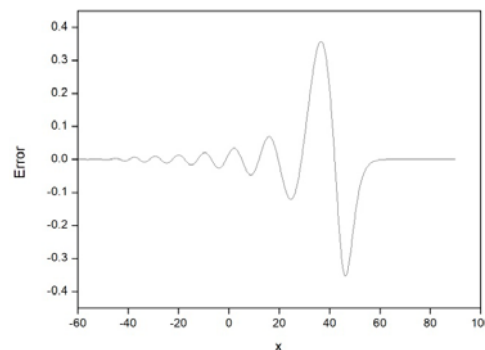


Figure 4. Absolute error for $p = 3$, $\alpha = 1$, $\beta = 1$, $\varepsilon = 1$, $h = \Delta t = 0.125$ at $t = 40$.

5.1.3. CASE 3

For the third case, we have taken the parameters $p = 5$, $\alpha = 1$, $\beta = 1$, $\varepsilon = 1$ over the interval $[-60, 90]$. For this set the exact solution of the equation can be obtained as [4, 9]

$$U(x, t) = \sqrt[4]{\frac{4}{15}(-5 + \sqrt{34})} \operatorname{sech} \frac{1}{3} \sqrt{-5 + \sqrt{34}} \left[x - \frac{1}{10} (5 + \sqrt{34}) t \right].$$

We search the equation with the boundary conditions $U \rightarrow 0$ as $x \rightarrow \pm\infty$ and the initial condition

$$U(x, 0) = \sqrt[4]{\frac{4}{15}(-5 + \sqrt{34})} \operatorname{sech} \frac{1}{3} \sqrt{-5 + \sqrt{34}} x.$$

For these parameters, the solitary wave has an amplitude 0.686098 and the run of the algorithm is activated to time $t = 40$ to get the invariants and error norms at various times. The velocity of the solitary wave is $v = 1.083095$. The obtained results are reported in Table (6). The percentage of the relative error of the preserved quantities I_M and I_E are calculated with respect to the preserved quantities at $t = 0$. The percentage of relative changes of I_M and I_E are found to be $1.4 \times 10^{-4}\%$ and $1.2 \times 10^{-8}\%$ for $h = \Delta t = 0.25$; $8.6 \times 10^{-5}\%$ and $5.0 \times 10^{-10}\%$ for $h = \Delta t = 0.125$; $7.0 \times 10^{-5}\%$ and $2.8 \times 10^{-9}\%$ for $h = \Delta t = 0.0625$, respectively. Table (6) indicates that invariants are nearly constant as the time progresses. As one can see straightforwardly from the table that the invariants I_M and I_E change from their initial value by less than 1.0×10^{-9} for different values of h and Δt . Also, we have found out error norms L_2 and L_∞ are obtained sufficiently small during the computer run. Thus, we can say our method is marginally conservative. For comparison purpose, the values of the L_∞ error norms are presented in comparison with M. Zheng et al. [10] and Y. Luo et al. [11] in Table (7). It is obviously seen from this table, the error norms obtained by our method are much better than the others again. The numerically computed results of the I_E are compared with [11] in Table (8). Results show that the values of the invariant are to be very close to each other. The behaviours of solutions for values of $h = \Delta t = 0.125$ at times $t = 0, 20$ and 40 are depicted in Figure (5). Figure (5) shows that the suggested method execute the motion of propagation of a solitary wave satisfactorily, which moves to the right at a constant speed and nearly preserves its amplitude and shape with increasing time. The amplitude is 0.686098 at $t = 0$ and located at $x = 0$, while it is 0.685675 at $t = 40$ and located at $x = 43.250$. The absolute difference in amplitudes at times $t = 0$ and $t = 40$ is 4.2×10^{-4} so there is a little change between amplitudes. The error graph at $t = 40$ is shown in Figure (6). It is seen that the maximum errors are about the tip of the solitary waves and between -1.5×10^{-3} and 1.5×10^{-3} .

Table 6. The invariants and the error norms for single solitary wave with $p = 5$, $\alpha = 1$, $\beta = 1$, $\varepsilon = 1$.

$h = \Delta t = 0.25$	I_M	I_E	$L_2 \times 10^{-3}$	$L_\infty \times 10^{-3}$
t				
0	7.0936435935	3.1107124064	0	0
10	7.0936434216	3.1107124063	4.153031	1.693890
20	7.0936429528	3.1107124062	8.102177	3.110721
30	7.0936419009	3.1107124061	12.123006	4.503564
40	7.0936330521	3.1107124060	16.299008	5.925606
$h = \Delta t = 0.125$				
t				
0	7.0936435925	3.1107124063	0	0
10	7.0936434493	3.1107124063	1.042200	0.425642

20	7.0936431881	3.1107124063	2.035122	0.781637
30	7.0936426572	3.1107124063	3.047657	1.132638
40	7.0936374525	3.1107124064	4.100587	1.493427

Table 6. (continued)

$h = \Delta t = 0.0625$				
t				
0	7.0936435920	3.1107124063	0	0
10	7.0936434618	3.1107124063	0.260777	0.106504
20	7.0936432752	3.1107124063	0.509351	0.195642
30	7.0936429006	3.1107124062	0.762935	0.283659
40	7.0936386078	3.1107124063	0.102671	0.373985

Table 7. Comparison of error norms with $p = 5$, $\alpha = 1$, $\beta = 1$, $\varepsilon = 1$ and different values of h and Δt at time $t = 40$.

	$L_\infty \times 10^{-3}$		
	Present	[10]	[11]
$h = \Delta t = 0.25$	5.92560	17.9985	12.0204
$h = \Delta t = 0.125$	1.49342	4.56804	3.03743
$h = \Delta t = 0.0625$	0.37398	1.14689	0.76141

Table 8. Comparison of I_E with $p = 5$, $\alpha = 1$, $\beta = 1$, $\varepsilon = 1$ and different values of h and Δt .

$h = \Delta t = 0.25$	I_E	I_E
t	Present	[11]
0	3.1107124064	3.11067490241
10	3.1107124063	3.11067490241
20	3.1107124062	3.11067490240
30	3.1107124061	3.11067490240
40	3.1107124060	3.11067490240
$h = \Delta t = 0.125$		
t	Present	[11]
0	3.1107124063	3.11070293879
10	3.1107124063	3.11070293879
20	3.1107124063	3.11070293879
30	3.1107124063	3.11070293879
40	3.1107124064	3.11070293879
$h = \Delta t = 0.0625$		
t	Present	[11]
0	3.1107124063	3.110702996431
10	3.1107124063	3.110702996430
20	3.1107124063	3.110702996426
30	3.1107124062	3.110702996417
40	3.1107124063	3.110702996435

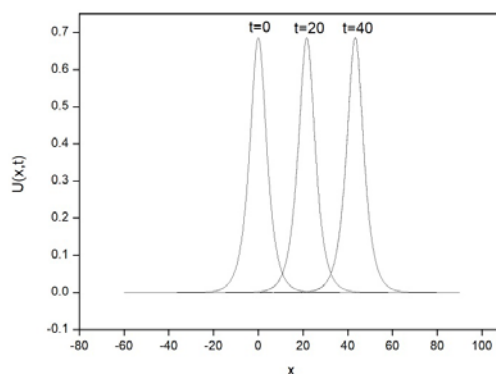


Figure 5. Motion of single solitary wave for $p = 5$, $\alpha = 1$, $\beta = 1$, $\varepsilon = 1$, $h = \Delta t = 0.125$ over the interval $[-60; 90]$ at specified times.

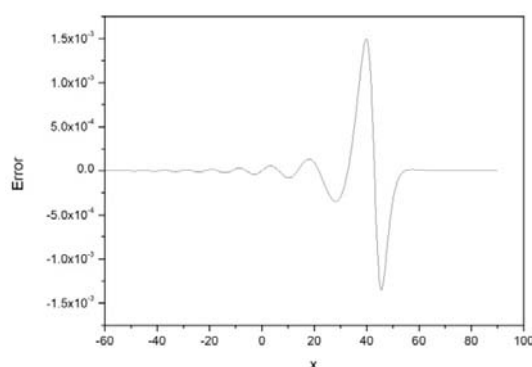


Figure 6. Absolute error for $p = 5$, $\alpha = 1$, $\beta = 1$, $\varepsilon = 1$, $h = \Delta t = 0.125$ at $t = 40$.

CONCLUSION

In this paper, we have successfully implemented septic B-spline collocation finite element method for the numerical solutions of the nonlinear generalized Rosenau-KdV equation. For single solitary wave, to prove the performance of the numerical algorithm, the error norms L_2 , L_∞ and the invariants I_M and I_E have been calculated. These calculations shows that our error norms are sufficiently small and they are smaller than or too close to the ones in existing numerical results. The changes of the invariants are adequately small and the quantities of the invariants are consistent with those of [2, 6, 11]. Also, stability analysis has been done and the linearized scheme has been found to be unconditionally stable. The obtained results show that the collocation method using septic B-spline shape functions is a remarkably successful numerical technique for solving the generalized Rosenau-KdV equation and can also be efficiently applied to a broad class of physically important non-linear partial differential equations.

REFERENCES

- [1] Zuo, J.M., *Applied Mathematics and Computation*, **215**, 835, 2009.
- [2] Hu, J., Xu, Y., Hu, B., *Advances in Mathematical Physics*, **2013**, Article ID 423718, 2013.
- [3] Ebadi, G., Mojaver, A., Triki, H., Yildirim, A., Biswas, A., *Romanian Journal of Physics*, **58**(1-2), 3, 2013.
- [4] Razborova, P., Triki, H., Biswas, A., *Ocean Engineering*, **63**, 1, 2013.
- [5] Wongsajjai, B., Poochinapan, K., *Applied Mathematics and Computation*, **245**, 289, 2014.
- [6] Ak, T., Karakoc, S.B.G., Triki, H., *Eur. Phys. J. Plus.*, **131**, 356, 2016.
- [7] Ak, T., Dhawan, S., Karakoc, S.B.G., Bhowmik, S.K., Raslan, K.R., *Mathematical Modelling and Analysis*, **22**(3), 373, 2017.
- [8] Atouani, N., Omrani, K., *Applied Mathematics and Computation*, **250**, 832, 2015.
- [9] Esfahani, A., *Commun. Theor. Phys.*, **55**, 396, 2011.
- [10] Zheng, M., Zhou, J., *Journal of Applied Mathematics*, **2014**, Article ID 202793, 2014.
- [11] Luo, Y., Xu, Y., Feng, M., *Advances in Mathematical Physics*, **2014**, Article ID 986098, 2014.
- [12] Korteweg, D.J., de Vries, G., *Philosophical Magazine*, **39**, 422, 1895.
- [13] Ak, T., Karakoc, S.B.G., Biswas, A., *Iranian journal of Science and Technology, Transactions A: Science*, **41**(4), 1109, 2017.
- [14] Pan, X., Zhang, L., *Applied Mathematics and Computation*, **218**, 8917, 2012.
- [15] Rosenau, P., *Phys. Scripta*, **34**, 827, 1986.
- [16] Rosenau, P., *Progr. Theory. Phys.*, **79**, 1028, 1988.
- [17] Park, M.A., *Math. Appl. Comput.*, **9**, 145, 1990.
- [18] Prenter, P.M., *Splines and Variational Methods*. John Wiley & Sons, New York, 245 1975.
- [19] Zeybek, H., Karakoc, S.B.G., *Electronic Transactions on Numerical Analysis*, **46**, 71, 2017.
- [20] Bochev, P.B., Gunzburger, M.D., *Least-squares finite element methods*, Springer, New York, 189, 2009.
- [21] Suli, E., Mayers, D.F., *An introduction to numerical analysis*, Cambridge University Press, New York, 293, 2003.
- [22] Thomee, V., *Galerkin finite element methods for parabolic problems*, Springer Berlin Heidelberg New York, 81, 2006.